DETERMINATION OF THE IMPACT OF THE GRAIN SIZE AND THE RECOMBINATION VELOCITY AT GRAIN BOUNDARY ON THE VALUES OF THE ELECTRICAL PARAMETERS OF A BIFACIAL POLYCRISTALLIN SILICON SOLAR CELL

M. M. Dione[1], I. Ly[2], A. Diao[1], S. Gueye[1], A. Gueye[1], M. Thiame[1], G. Sissoko[1] (Corresponding Author: G. Sissoko, gsissoko@yahoo.com)

[1]Laboratory of Semiconductors and Solar Energy, Physics Departement, Faculty of Sciences and Technology, University Cheikh Anta Diop, Dakar, Senegal
[2]Ecole Polytechnique of Thies, EPT, Thies, Senegal

Abstract: Our objective in this study is to analyse the impact of the grain size and recombination velocity at grain boundary on the electrical parameter. After the resolution of the continuity equation the expression of photocurrent density and photovoltage are presented and the curve of the I-V characteristic is plotted; two equivalents electric circuit of the solar cell in open and short circuit are proposed allowing us to deduce the shunt and series resistance and their values respectively for large and low values of the grain size and recombination velocity at grain boundary.

Keywords: *shunt resistance – series resistance – grain size – recombination velocity at grain boundary*

I - INTRODUCTION

Several characterization techniques of silicon material, determination of phenomenological and electrical parameters have been used to improve the ability of solar cells. Some of these techniques have been developed under static conditions [1] and others in dynamic frequency [2]. Extensive studies on the ability of the space charge region [3, 4, 5], recombination parameters [6, 7], as well as other parameters in the presence [2, 3, 8, 9, 10, 11] or without a magnetic field were performed three dimensions [7, 8, 11, 12, 13, 14] for these two regimes.

In this study we are led to identify and analyze the effect of recombination velocity at grain boundaries and grain size on the electrical parameters of a polycrystalline silicon solar cell under static conditions and under constant polychromatic illumination.

II-THEORY

The polycrystalline substrate is composed of several grains of various shapes and sizes. For this study three-dimensional modeling, we use a model where the columnar grain is represented by a parallelepiped according to the following figure. [12]

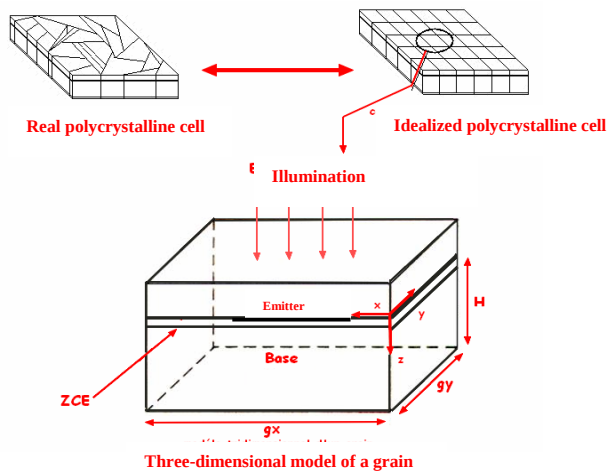

Figure 1: Modeling a polysilicon grain

In the framework of our study, we make the following approximations [7] :

i) The contribution of the transmitter will be neglected in comparison with that of the base.

ii) The crystal field is neglected at the base of the solar cell, only the electric field at the junction will be taken into account.

iii) We use a three-dimensional mathematical model of the solar cell, the joint will be taken as the origin (x = 0).

iv) The illumination will be along the axis z.

II.1 Continuity equation

The continuity equation which governs the phenomena of recombination and diffusion in the base of the solar cell is given by equation (1):

$$\left(\frac{\partial^2}{\partial x^2}+\frac{\partial^2}{\partial y^2}+\frac{\partial^2}{\partial z^2}\right)n(x,y,z)-\frac{n(x,y,z)}{L_n{}^2}=-\frac{G_n(z)}{D_n} \quad \textbf{(1)}$$

where n (x, y, z) is the minority carrier density at the base, and L_n and D_n represent the length and the diffusion coefficient of electrons in the base. In this expression, G_n (z) is the generation rate and is given by the following equation [15]:

$$G_n(z) = \sum_{\lambda_0}^{\lambda_g} \alpha_\lambda \cdot F_{0\lambda}\left(1 - r_\lambda\right) \cdot e^{\alpha_\lambda \cdot z} \quad \textbf{(2)}$$

where α, r_λ, $F_{0\lambda}$ represent respectively the absorption coefficient, the light flux and the reflection coefficient at the wavelength λ, while λ_0 and λ_g respectively denote the lengths of the maximum and minimum cut-off of the light source [15].

The general solution of the continuity equation is given by the expression (3) as follows:

$$n(x, y, z) = \sum_k \sum_j \cos(c_k \cdot x) \cdot \cos(c_j \cdot y) \cdot Z_{kj}(z) \quad \textbf{(3)}$$

The coefficients C_k and C_j solutions are obtained with clean space resolution transcendental equations which are given by the boundary conditions at the grain boundaries as follows:

$$D_n \cdot \left.\frac{\partial n(x, y, z)}{\partial y}\right|_{y=\pm\frac{gy}{2}} = \mp S_{gb} \cdot n(x, y, z)\Big|_{y=\pm\frac{gy}{2}} \quad \textbf{(4)}$$

$$D_n \cdot \left.\frac{\partial n(x, y, z)}{\partial x}\right|_{x=\pm\frac{gx}{2}} = \mp S_{gb} \cdot n(x, y, z)\Big|_{x=\pm\frac{gx}{2}} \quad \textbf{(5)}$$

G_{BS} is the recombination velocity at grain boundaries.

With the resolution of transcendental equations we obtain the eigenvalues C_k and C_j. Expressions of these equations are given by equations (6) and (7):

$$c_k \cdot \tan\left(c_k \cdot \frac{gx}{2}\right) = \frac{S_{gb}}{D_n} \quad \textbf{(6)}$$

$$c_j \cdot \tan\left(c_j \cdot \frac{gy}{2}\right) = \frac{S_{gb}}{D_n} \quad \textbf{(7)}$$

Putting the general solution of our equation of continuity in the expression (1), we obtain the new equation given by:

$$\frac{\partial^2 Z_{kj}(z)}{\partial z^2} - \frac{1}{{L_{kj}}^2} Z_{kj}(z) = -\frac{1}{D_{kj}} \sum_{\lambda_0}^{\lambda_g} N_0 \cdot e^{-\alpha_\lambda \cdot z} \quad \textbf{(8)}$$

with :

$${c_k}^2 + {c_j}^2 + \frac{1}{{L_n}^2} = \frac{1}{{L_{kj}}^2} \quad \textbf{(9)}$$

$$D_{kj} = \frac{\left(c_k \cdot gx + \sin(c_k \cdot gx)\right) \cdot \left(c_j \cdot gy + \sin(c_j \cdot gy)\right)}{16 \sin\left(c_k \cdot \frac{gx}{2}\right) \cdot \sin\left(c_j \cdot \frac{gy}{2}\right)} \quad \textbf{(10)}$$

$$N_0 = \frac{\left(1 - r_\lambda\right)\alpha_\lambda \cdot F_{0\lambda}}{D_n} \quad \textbf{(11)}$$

L_{kj} and D_{kj} represent the length and the effective diffusion coefficient. The solution of equation (8) is given by:

$$Z_{kj}(z) = A_{kj} \cdot \cosh\left(\frac{z}{L_{kj}}\right) + B_{kj} \cdot \sinh\left(\frac{z}{L_{kj}}\right) + \sum_{\lambda_0}^{\lambda_g} K_\lambda \cdot e^{-\alpha_\lambda \cdot z} \quad \textbf{(12)}$$

where :

$$K_\lambda = -\frac{N_0}{D_{kj}\left(\alpha_\lambda^2 - \frac{1}{L_{kj}^2}\right)} \quad \textbf{(13)}$$

A_{kj} and B_{kj} are constants to be determined using the boundary conditions at the junction and the rear whose expressions are given by:

At the junction:

$$D_n \cdot \left.\frac{\partial n(x, y, z)}{\partial z}\right|_{z=0} = S_F \cdot n(x, y, z)\Big|_{z=0} \quad \textbf{(14)}$$

At the rear:

$$D_n \cdot \left.\frac{\partial n(x, y, z)}{\partial z}\right|_{z=H} = -S_B \cdot n(x, y, z)\Big|_{z=H} \quad \textbf{(15)}$$

S_B and S_F denote the surface recombination velocity at the rear and at the junction. It should be noted that S_F is the sum of two contributions: S_{F0} [7] which is the intrinsic recombination velocity at the junction induced by losses in the shunt resistance and S_{FJ} [7] which reflects the current flow imposed by imposing an external load to the operating point of the solar cell. Its expression is given by equation (16):

$$S_F = S_{F0} + S_{FJ} \quad (16)$$

III RESULTS AND DISCUSSION

III.1 Photocurrent density

The photocurrent density is given by the average of the surface gx.gy local expression J_{ph}:

$$J_{ph} = \frac{4 \cdot q \cdot D_n}{gx \cdot gy} \int_{-\frac{gx}{2}}^{\frac{gx}{2}} \int_{-\frac{gy}{2}}^{\frac{gy}{2}} \left[\frac{\partial n(x,y,z)}{\partial z} \right]_{z=0} dx \cdot dy \quad (17)$$

Putting in this relationship the expression of the density of minority carriers in the base, we get the mathematical formula giving the photocurrent density generated. And in the same vein we have shown at figure 2, the evolution of the density function of the recombination velocity at the junction S_F.

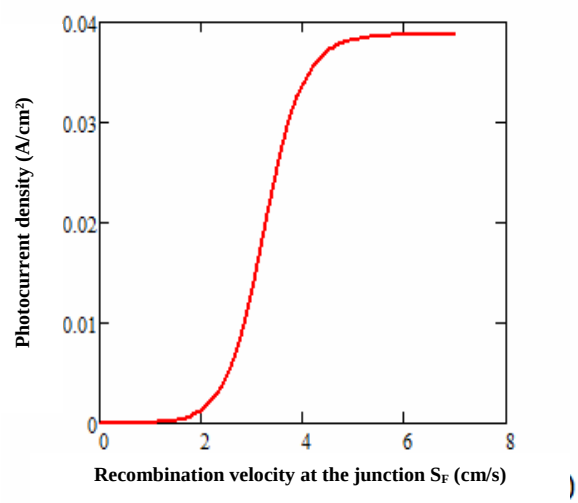

Figure 2: Profile of the photocurrent density based on the recombination velocity at the junction (D = 26 cm/s ² ; L = 0.02 cm; gx = gy = 0.01 cm ; S_{GB} = 400 cm/s ; S_B = 3000 cm/s)

We note in this figure that the photocurrent density is an increasing function of the rate of recombination at the junction. For high values of S_F ie when one is in a situation of short-circuit, photocurrent approaches a limit which represents the short-circuit and the carrier density is almost zero since there are more charge carriers to the junction. And at low values of S_F, there is a blockage and storage of carriers, this translates into the fact that there is no passage of carriers at the junction, so no current: it is thus in a position of open circuit.

III.2.Photovoltage

It characterizes the potential barrier present at the emitter-base junction. Its expression is given by the average (on the surface gx.gy) of the minority carrier density at the junction ie at x = 0 cm.

$$V_{ph} = V_T \cdot \ln\left[1 + \frac{N_B}{n_i^2} \cdot \int_{-\frac{gx}{2}}^{\frac{gx}{2}} \int_{-\frac{gy}{2}}^{\frac{gy}{2}} \left[\frac{\partial n(x,y,z)}{\partial z} \right]_{z=0} dx \cdot dy \right] \quad (18)$$

where V_T is the thermal voltage, N_B and n_i represent respectively the doping level of the base and the impurity atom concentration of carriers in intrinsic base.

At figure 3, we plot the profile of the photovoltage as a function of recombination velocity S_F.

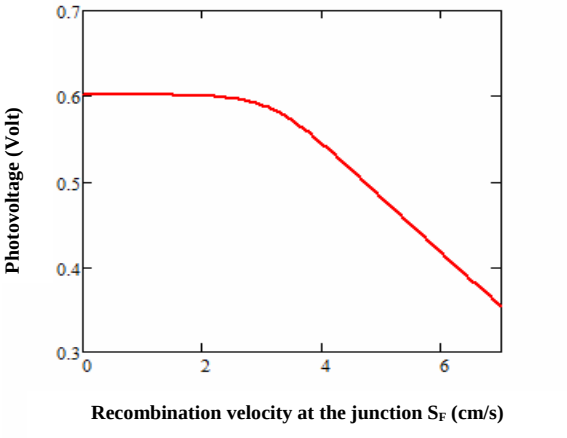

Figure 3: Profile of the photovoltage as a function of the recombination velocity at the junction (D = 26 cm/s ² ; L = 0.02 cm ; gx = gy = 0.01 cm ; S_{GB} = 400 cm/s ; S_B = 3000 cm/s)

The analysis of this curve shows that for high values of the recombination velocity S_F, photovoltage tends to zero because there are more carriers at the junction and for low values of this velocity, the fact that there is no flow of charge carriers, the photovoltage remains constant and corresponds to the open circuit voltage V_{CO}.

III.3 Characteristic current - voltage

Since the photovoltage and the photocurrent density are both functions of the recombination velocity at the junction S_F, we can represent the two quantities as a function of one another (ie the photocurrent density according to the photovoltage).

Hence, we obtain the current-voltage characteristic.

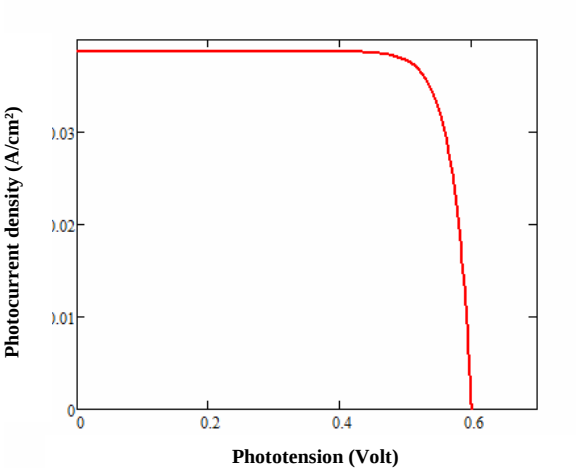

Figure 4: Current-voltage characteristic of the solar cell (D = 26 cm/s ² ; L = 0.02 cm; gx = gy = 0.01 cm ; S_{GB} = 400 cm/s; S_B = 3000cm/s)

III.4 Shunt resistance :

From the run - voltage characteristic of the solar cell, we can notice that to the neighborhood of the short circuit (figure 5), the solar cell behaves like a generator of current because the produced current is practically independent of voltage to its boundary-marks.

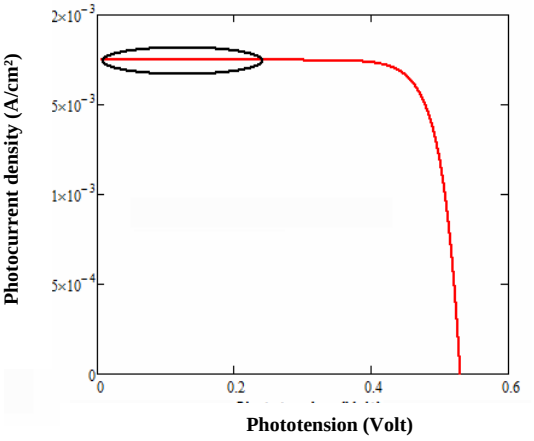

Figure 5: Current-voltage characteristics

For an ideal solar cell, this branch of the characteristic is perfectly horizontal because the produced current is really constant some either voltage to the limit. Actually, for a non ideal solar cell a generally weak flight current that causes a very small variation of the current produced by the solar cell exists when its voltage to the boundary-marks varies, what translates the presence of an internal load to the solar cell that one calls leakage resistance or resistance shunt [16]. To the figure 6, we propose an equivalent electric circuit of the solar cell when this one operates practically in short circuit [8, 10, 17, 18, 19].

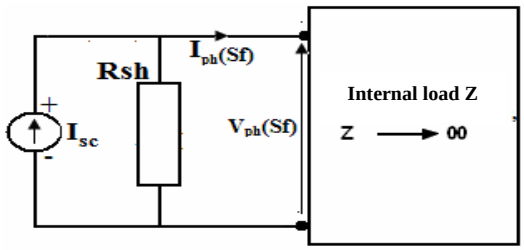

Figure 6: Equivalent circuit of a solar cell short circuit

From the stitch that involves the load resistance, we get the following equation: $V_{ph} = R_{SH}\left(J_{CC} - J_{ph}\right)$ **(19)**

what leads to the following expression of the shunt resistance:

$$R_{SH} = \frac{V_{PH}}{J_{CC} - J_{PH}} \qquad \textbf{(20)}$$

From this expression, we gave to the follow figures the evolution of the shunt resistance according to the recombination velocity S_F for various values of the recombination velocity to the joints of grain and size of grain.

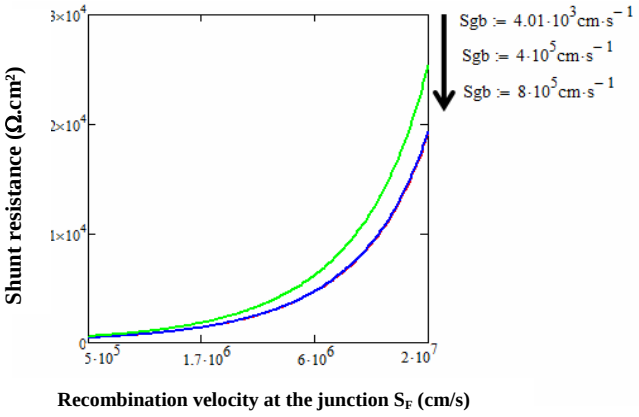

Figure 7: Profile of the shunt resistance as a function of the recombination velocity at the junction (D = 26 cm/s ² ; L = 0.02 cm; gx = gy = 0.01 cm ; S_B = 3000 cm/s)

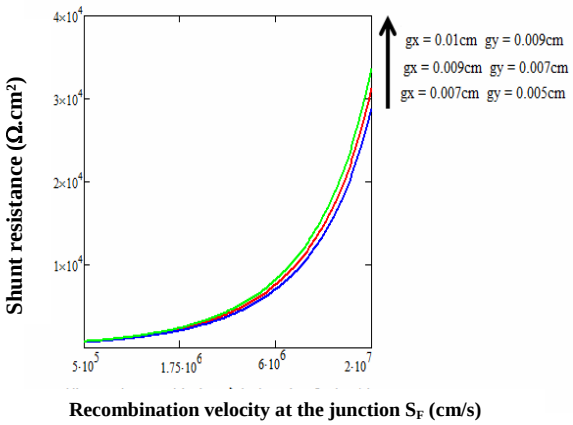

Figure 8: Profile of the shunt resistance as a function of the recombination velocity at the junction (D = 26 cm/s ² ; L = 0.02 cm ; S_{GB} = 400 cm/s; S_B = 3000 cm/s)

Of the analysis of these graphs one pulls of it that the increase of the recombination velocity to the joints of grain comes with a reduction of the resistance shunt of the cell what explains themselves by the fact that the recombination activities of the grain joints increases the leakage current of the polycrystalline solar cell and decrease the photocourant therefore; while an increase of the grain size appears by a reduction of the leakage current, so a growth of the value of the shunt resistance what improves the performance of the solar cell.

III.5.1 Determination of the value of the shunt resistance

Determining the value of R_{SH} [21, 22] passes through that of the recombination velocity at the junction in short circuit S_{FCC} which is obtained by solving the following equation:

$$J_{PH}(S_F, S_B, S_{GB}, g) - J_{CC}(S_B, S_{GB}, g) = 0 \quad \textbf{(21)}$$

where the velocities S_{BS} and S_{GBS} are variable while the grain size g is fixed, and therefore this S_{FCC} velocity will be also function of these three quoted sizes.

	Recombination velocity S_{FCC}
gx = 0.007cm et gy = 0.005 cm S_{GB} = 4.01 10^4 cm/s	3.685 10^6
gx = 0.009 cm et gy = 0.007 cm S_{GB} = 4.01 10^4 cm/s	1.815 10^6
gx = 0.01 cm et gy = 0.009 cm S_{GB} = 8 10^5 cm/s	1.635 10^5

In the following table are given the different values of the recombination velocity to the junction in short circuit for different values of the size of grain and the S_{GB} velocity.

	Shunt Resistance R_{SH}
gx = 0.007 cm et gy = 0.005 cm S_{GB} = 4.01 10^4 cm/s	891.058
gx = 0.009 cm et gy = 0.007 cm S_{GB} = 4.01 10^4 cm/s	980.569
gx = 0.01 cm et gy = 0.009 cm S_{GB} = 8 10^5 cm/s	232.461

On the same thrown of the determination of the value of S_F in short circuit, we propose on following table a set of value of the shunt resistance corresponding to the S_{FCC} calculated previously for various sizes of grain and recombination velocities to the joints of grain.

III.5 Series resistance

As for the shunt resistance, we leave from current - voltage characteristic of the solar cell.

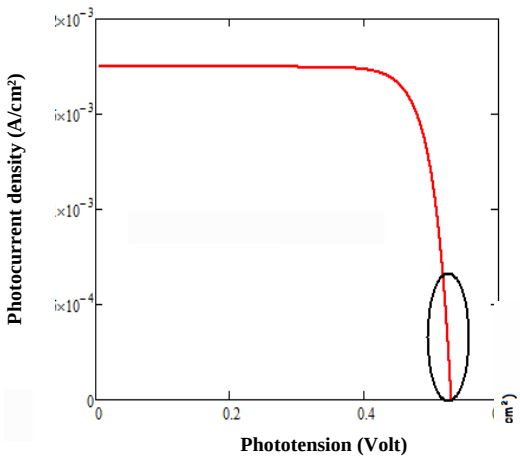

Figure 9: Current-voltage characteristic

We note that in the neighborhood of the o circuit, voltage to the boundary-marks of the s cell is practically independent of the produced current. The solar cell behaves then like a real voltage generator since its characteristic I-V is not identical to a vertical right. What explains the presence of an internal resistance due to the resistance of the polycristalline material that is not anything else that the series resistance of the solar cell [19, 20]. We propose to the following figure an equivalent electric circuit of the solar cell then when this one operates practically in open circuit [8, 10, 17, 18, 21].

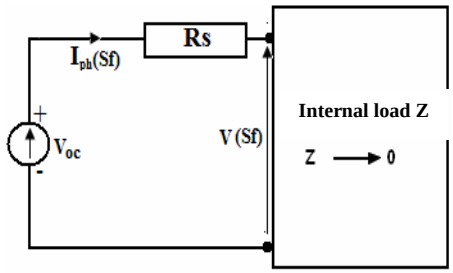

Figure 10: Equivalent circuit of a solar cell open circuit

As using the law of the stitches, we get the following equation:

$$V_{PH} = V_{CO} - R_S \cdot J_{PH} \qquad (22)$$

Hence, we get that:

$$R_S = \frac{V_{CO} - V_{PH}}{J_{PH}} \qquad (23)$$

And as leaving from this mathematical formula we represented to the following figures the variation of the series resistance according to the S_F velocity for various values of the recombination velocity to the joints of grain and the size of grain.

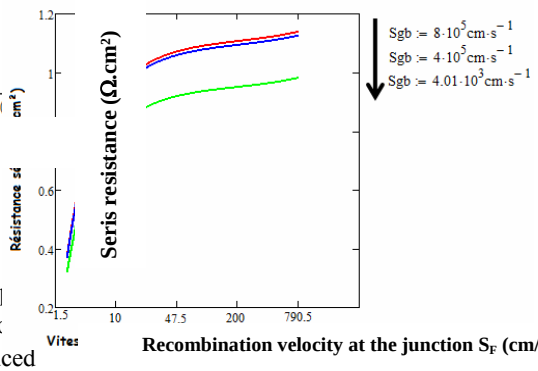

Figure 11: Profile of the series resistance depending on the rate of recombination at the junction (D = 26 cm/s ²; L = 0.02 cm; gx = gy = 0.01 cm; S_B = 3000 cm/s)

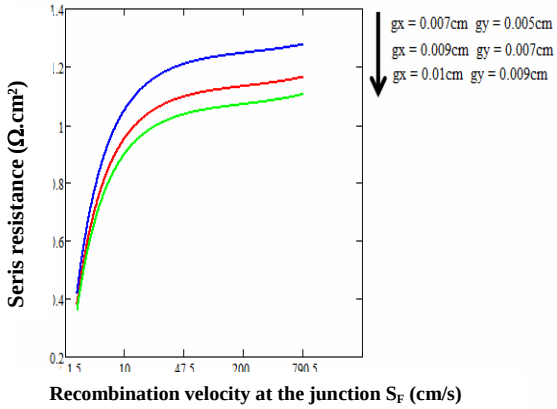

Figure 12: Profile of the series resistance depending on the rate of recombination at the junction (D = 26 cm/s ²; L = 0.02 cm; S_{GB} = 400 cm/s; S_B = 3000 cm/s)

The figures 11 and 12 illustrate the variations of the series resistance according to the recombination velocity in the junction S_F. And the analysis of these graphs reveals us that the series resistance increases when the recombination activities to the joints of grains intensify and this growth is of as much more marked that when the recombination velocity S_F is high. The speed of recombination to the joints of grain decreases voltage thus to the boundary-marks of the solar cell. The observation

of these same graphs also shows us that the series resistance is especially weak that the value of the grain size increases what results thus in a reduction of the recombination zones in the lively material a growth of the voltage amplitude to the boundary-marks of the solar cell.

III.5-1 Determination of the value of the series resistance

The determination of the series resistance will get used below through the intermediary of the calculation of the value of the recombination velocity to the junction in open circuit through the resolution of the equation:

$$V_{PH}(S_F, S_B, S_{GB}, g) - V_{CO}(S_B, S_{GB}, g) = 0 \quad \textbf{(24)}$$

Where the S_{BS} and S_{GBS} velocities are variable while the size grain g is fixed, and therefore this S_{FCO} velocity will also be function of these three quoted sizes.

	Recombination velocity S_{FCO}
gx = 0.007 cm et gy = 0.005 cm S_{GB} = 4.01 10^4 cm/s	177.045
gx = 0.009 cm et gy = 0.007 cm S_{GB} = 4.01 10^4 cm/s	87.022
gx = 0.01 cm et gy = 0.009 cm S_{GB} = 8 10^5 cm/s	31.777

To the level of the figure 3, we raised the values gotten at the time of the calculation of S_{FCO} for various values of the size of grain and the recombination velocity S_{GB}.

	Series resistance R_S
gx = 0.007 cm et gy = 0.005 cm S_{GB} = 4.01 10^4 cm/s	1.335
gx = 0.009 cm et gy = 0.007 cm S_{GB} = 4.01 10^4 cm/s	0.868
gx = 0.01 cm et gy = 0.009 cm S_{GB} = 8 10^5 cm/s	5.18

IV CONCLUSION

In this work we made a three-dimensional modeling of a solar cell to the polysilicon in static regime and under constant polychromatic illumination that permitted us to study the density of photocurrent, the photovoltage and current - voltage characteristic; and thereafter to put in evidence influences of the size of grain and the recombination velocity to the joints on the electrical parameters to know the shunt and series resistances. It was also evident from this survey that an increase of the grain size as well as a reduction of the recombination velocity to the joints improved the quality of the solar cell by an increase of the value of the flight resistance and a decrease of the one of the series resistance.

BIBLIOGRAPHIC REFERENCES

[1] M. M. DIONE, S. MBODJI, M. L. SAMB, M. DIENG, M. THIAME, S. NDOYE, F. I. BARRO and G. SISSOKO
Vertical junction under constant multispectral light: Determination of recombination parameters.
Proceedings of the 24th European Photovoltaic Solar Energy Conference, september 2009, Hamburg, Germany, pp 465-468, 1CV.4.14.

[2] S. MBODJI**,** A. S. MAIGA, M. DIENG, A. WEREME and G. SISSOKO
Renoval charge technic applied to a bifacial solar cell under constant magnetic field.
GLOBAL JOURNAL OF PURE AND APPLIED SCIENCES VOL 16, NO. 4 2010: 469- 477.

[3] S. MADOUGOU, NZONZOLO, S. MBODJI**,** I.F. BARRO and G. SISSOKO
Bifacial silicon solar cell space charge region width determination by a study in modelling: effect of the magnetic field.
J.Sci.Vol.4, N°3 (2004) 116-123.

[4] F. I. BARRO, S. MBODJI, M. NDIAYE, E. BA and G. SISSOKO
Influence of grains size and grains boundaries recombination on the space-charge layer thickness z of emitter-base junction's n+-p-p+ solar cell.
Proceedings of the 23rd European Photovoltaic Solar Energy Conference (2008), pp 604-607.
DOI : 10.4229/23rdEUPVSEC2008-1CV.2.63.

[5] M. NDIAYE, A. DIAO, M. THIAME, M.M. DIONE, H. LY DIALLO, M.L. SAMB, I. LY, C. GASSAMA, S. MBODJI, F.I. BARRO and G. SISSOKO
3D Approach for a Modelling Study of the Diffusion Capacitance's Efficiency of the Solar Cell.
Proceedings of the 25th EU-PVSEC/5th WCPEC (2010) pp 484-487,1DV.2.55.

[6]M.L. SAMB, M. DIENG, S. MBODJI, B. MBOW, N. THIAM, F.I. BARRO and G. SISSOKO.
Recombination parameters measurement of silicon solar cell under constant white bias light.
Proceedings of the 24th European Photovoltaic Solar Energy Conference (2009), pp.469-472
DOI: 10.4229/24th EUPVSEC2009-1CV.4.15.

[7] H. L. DIALLO, A. S. MAIGA, A. WEREME, G. SISSOKO
New approach of both junction and back surface recombination velocity in a 3D modelling study of a polycrystalline silicon solar cell.
Eur. Phys. J. Appl. Phys. 42, 203-211 (2008)

[8] A. DIENG, M.L. SOW, S. MBODJI, M.L. SAMB, M. NDIAYE, M. THIAME, F.I. BARRO and G. SISSOKO
3D Study of a Polycrystalline Silicon Solar Cell: Influence of Applied Magnetic Field on the Electrical Parameters.
Proceedings of the 24th European Photovoltaic Solar Energy Conference (2009), pp .473-476
DOI: 10.4229/24th EU-PVSEC 2009-1CV.4.16.

[9] S. MADOUGOU, NZONZOLO, S. MBODJI, I. F. BARRO, G. SISSOKO
Bifacial silicon solar cell space charge region width determination by a study in modelling : Effect of the magnetic field.
J.Sci.Vol.4, N°3 (2004) 116-123.

[10] S. MADOUGOU, F. MADE, M. S. BOUKARY, and G. SISSOKO
I-V Characteristics for Bifacial Silicon Solar Cell studied under a Magnetic field.
Advanced Materials Research Vols. 18-19 (2007) pp. 303-312

[11] B. ZOUMA, A. S. MAIGA, M. DIENG, F. ZOUGMORE, G. SISSOKO
3D Approach of spectral response for a bifacial silicon solar cell under a constant magnetic field.
Global Journal of Pure and Applied Sciences, Vol.15, N°1, 2009, pp.117-124.

[12] J. Dugas, Solar Energy Materials and Solar Cells, 32 (1994), pp.71-88.

[13] S.MBODJI, B.MBOW, F.I.BARRO and G.SISSOKO
A 3D model for thickness and diffusion capacitance of emitter-base junction in a bifacial polycrystalline solar cell.
Global Journal of Pure and Applied Sciences Vol 16, No.4, 2010.

[14] S.MBODJI**,** M.DIENG, B.MBOW, F.I.BARRO and G.SISSOKO
Three dimensional simulated modeling of diffusion capacitance of polycrystalline bifacial silicon solar cell.
Journal of Applied Sciences and Technology (JAST) Vol. 15, Nos.1&2, 2010, pp 109 – 114.

[15] J.D. ARORA, S.N. SINGH, P.C. MATHUR
Solid State Electronics Vol 24, No.8, pp 739-747, 1981

[16]JEAN-PIERRE CHARLES, AHMED HADDI, ALAIN MAOUAD, HAZRI BAKHTIAR, ABDELLATIF ZERGA, ALAIN HOFFMANN, PIERRE MIALHE.
La Jonction, du Solaire à la Microélectronique
Revue des Energies Renouvelables, Vol.3 (2000)1-16

[17]F. I. BARRO, S. GAYE, M. DEME, H. L. DIALLO, M. L. SAMB, A. M. SAMOURA, S. MBODJI and G. SISSOKO
Influence of grain size and grain boundary recombination velocity on the series and shunt resistances of a polycrystalline silicon solar cell.
Proceedings of the 23rd European Photovoltaic Solar Energy Conference(2008), pp 612-615.
DOI : 10.4229 / 23rd EUPVSEC 2008-1CV.2.65.

[18] S. MBODJI, H. LY.DIALLO**,** I.LY, A.DIOUM, I.F.BARRO and G. SISSOKO
Equivalent Electric circuit of a bifacial solar cell in transient state under Constant magnetic field.
Proceedings of the 21st European Photovoltaic Solar Energy Conference (2006), pp. 447 - 450

[19] E. CÁNOVAS, A. MARTÍ AND A. LUQUE
Design of circular symmetry metal grid patterns for concentration solar cells.
Proceedings of the 21st European Photovoltaic Solar Energy Conference (2006), pp. 389 -395

[20] K. KOTSOVOS AND K. MISIAKOS
Evaluation of series resistance losses in the base of single and double junction rear point contact silicon solar cells through simulation and experiment.
Proceedings of the 21st European Photovoltaic Solar Energy Conference (2006), pp.328 – 331

[21] M.M. DIONE, H. LY DIALLO, M. WADE, I. LY, M. THIAME, F. TOURE, A. GUEYE CAMARA, N. DIEME, Z. NOUHOU BAKO, S. MBODJI, F. I BARRO, G. SISSOKO
Determination of the shunt and series resistances of a vertical multijunction solar cell under constant multispectral light.
Proceedings of the 26th European Photovoltaic Solar Energy Conference (2011)-1CV.6
pp : 2 5 0 - 2 5 4 , D O I :10.4229 / 26th EUPVSEC 2011-1CV.3.6.

[22] I. LY, M. NDIAYE, M. WADE, N. THIAM, S. GUEYE, G. SISSOKO.
Concept of recombination velocity Sfcc at the junction of a bifacial silicon solar cell, in steady state, initiating the short-circuit condition.
Research Journal of Applied Sciences, Engineering and Technology (RJASET) 5(1) (2013) 203-208.